SCIENCE CHINA
Technological Sciences

•Article•

May 2020 Vol.63 No.5: 731–739
https://doi.org/10.1007/s11431-019-1446-0

Microstructure and bioactivity of a cold sprayed rough/porous Ta coating on Ti6Al4V substrate

TANG JunRong[1,2], ZHAO ZhiPo[1,2], CUI XinYu[1], WANG JiQiang[1*] & XIONG TianYing[1*]

[1] *Institute of Metal Research, Chinese Academy of Sciences, Shenyang 110016, China;*
[2] *School of Materials Science and Engineering, University of Science and Technology of China, Shenyang 110016, China*

Received May 15, 2019; accepted September 16, 2019; published online January 14, 2020

To improve the bioactivity and biocompatibility of titanium implants, a rough/porous tantalum (Ta) coating was firstly prepared on Ti6Al4V substrate by cold spraying. The results indicated that the surface of Ta coating is extremely rough with lots of visible holes, because of poor deposition quality. Microstructure and microhardness results showed that different layers appeared in the inner and outer parts of coatings, corresponding to porosity, due to lack of subsequent compaction. The simulated body fluid (SBF) soaking test showed that spherical apatite sediments were mineralized on rough/porous surface in SBF after 2–4 weeks, which demonstrated that the cold sprayed Ta coating had good bioactivity. This was mainly attributed to the rough/porous surface of Ta coating obtained by cold spraying, which is conducive to the heterogeneous nucleation of apatite on it.

cold spray, tantalum coatings, SBF soaking test, bioactivity

Citation: Tang J R, Zhao Z P, Cui X Y, et al. Microstructure and bioactivity of a cold sprayed rough/porous Ta coating on Ti6Al4V substrate. Sci China Tech Sci, 2020, 63: 731–739, https://doi.org/10.1007/s11431-019-1446-0

1 Introduction

With more and more orthopedic diseases [1,2], people are trying to find effective ways to repair human bone. Metallic biomaterials are extremely crucial for fracture fixation, bone repair and failed tissue, especially failed hard tissue, to improve patients' quality of life [3,4]. Conventional implant materials such as stainless steels, Co-Cr alloys, Ti and its alloys have been widely used in the medical field for many years [3,5]. The one of most frequent designs for Ti alloys implants is hip prosthesis [3,6]. Among them, Ti6Al4V has been widely studied [7,8] because of the high strength and toughness, low density and good corrosion resistance. It is well known that bioactive materials form bioactive bonding with the living bone by forming an apatite layer on their surfaces after they are implanted in the bony site [9]. Nevertheless, biological properties of the above materials are still far from being what humans require. Their bio-functionality is at present inadequate and a fibrous layer may form at the skeletal tissue/device interface causing aseptic loosening of the device [10]. Besides, these materials can potentially cause some health problems because of the release of toxic metal ions [11]. Hence, the biocompatibility of metallic biomaterials requires much improvement [12,13]. To solve these existing problems, there is a significant demand for carrying out surface modification to enhance the osteogenesis capacity for implants.

In recent years, tantalum (Ta) is gaining increasing interest for its excellent biocompatibility [14,15]. Ta is considered as one of the promising materials in promoting osseointegration [16–18]. It has excellent chemical properties owing to the stable tantalum pentaoxide (Ta_2O_5) protective film [19,20]. The excellent biocompatibility and superior corrosion resistance of pure Ta have been extensively evaluated and recognized by many medical researchers [21–23]. As early as 1940, Burke [21] successfully introduced pure Ta for surgi-

*Corresponding authors (email: jqwang11s@imr.ac.cn; tyxiong@imr.ac.cn)

cal implants such as sutures, bone screws and plates. What is more, Ta can be adapted to biological cells with excellent affinity, hardly stimulation and side effects in direct contact with human bone, muscle tissue and liquid [24,25].

However, since Ta is a heavy refractory metal with excellent high melting point (approximately 3000°C) and powerful affinity for oxygen [26,27], the fabrication of Ta has its particularity. Ta applications in biomedical devices have been limited by processing challenges rather than biological performance. Relatively high price of Ta further limits its application, too.

Therefore, compared with directly using bulk Ta, preparation of Ta coatings on the suitable and practical material is a promising solution. At present, Ta coatings are mainly prepared by chemical vapor deposition (CVD) on porous carbon skeleton [28], or powder sintering process [29]. There are also some other preparation methods, such as plasma spraying [30], sputter deposition [31] and laser engineered net shaping (LENS™) [32]. However, these methods have some drawbacks, such as high cost, high temperature and oxidation resulting in loss of ductility of metals. Thus high vacuum or high purity protective atmosphere is needed in order to avoid oxidation caused by the high temperature in the process of deposition.

Cold spraying was developed by employing a supersonic wind tunnel with tracer particles entrained in the high velocity gas stream in the mid-1980s at the Institute of Theoretical and Applied Mechanics, part of the Siberian Division of the Russian Academy of Science in Novosibirsk [33,34]. It is a kind of new technique based on the aerodynamics [35–37]. In the cold spraying process, a gas (compressed air, N_2 or even He) is accelerated to supersonic velocity carrying powders through convergent-divergent nozzle to produce supersonic gas-solid two-phase flow, and particles are deposited on the substrate via large plastic deformation in complete solid state [38,39]. Furthermore, the gas temperature at the inlet is clearly below the melting point of the coating material, which means the particles cannot be melted in the gas jet [38,39]. Compared with thermal sprayed coatings, the composition and microstructure of cold sprayed coatings are consistent with that of the raw material powders [40,41]. Therefore, cold spraying can avoid the performance degradation due to the high temperature which can result in undesirable phase transition and oxidation and is especially suitable for the preparation of the sensitive materials [42–44]. And that cold spraying as an emerging technology has been reported for biocompatible and antibacterial coatings [45].

According to the above analysis, cold spraying is a suitable method for preparing bioactive Ta coatings. However, only a few papers [46–49] reported the corrosion behavior of cold sprayed Ta coatings. There was almost no paper which studied the bioactivity of cold sprayed Ta coatings. A new direction of material development has been taken in the research of rough/porous coating surfaces for improving biological properties of hip and knee prosthesis [50]. Therefore, in this paper, a rough/porous Ta coating was fabricated by cold spraying and the microstructure and bioactivity of the coating were investigated.

2 Experimental

2.1 Materials

Commercially available hydride de-hydride Ta powders (Beijing DeKeDaoJin Technology Co. Ltd, China) were used in this experiment. The powders had a particle size of –41+13 μm (probed by a laser particle size analyzer), collected between 1000# and 400# mesh sieves. The surface morphology of Ta powders was observed using a scanning electron microscopy (SEM) (Figure 1). It indicated that the Ta powders had an irregular shape. The substrate material used in this study was Ti6Al4V. Prior to cold spray deposition, the substrate was ground by fine abrasive paper, cleaned with alcohol, and then sandblasted using SiO_2 grit (~24 mesh).

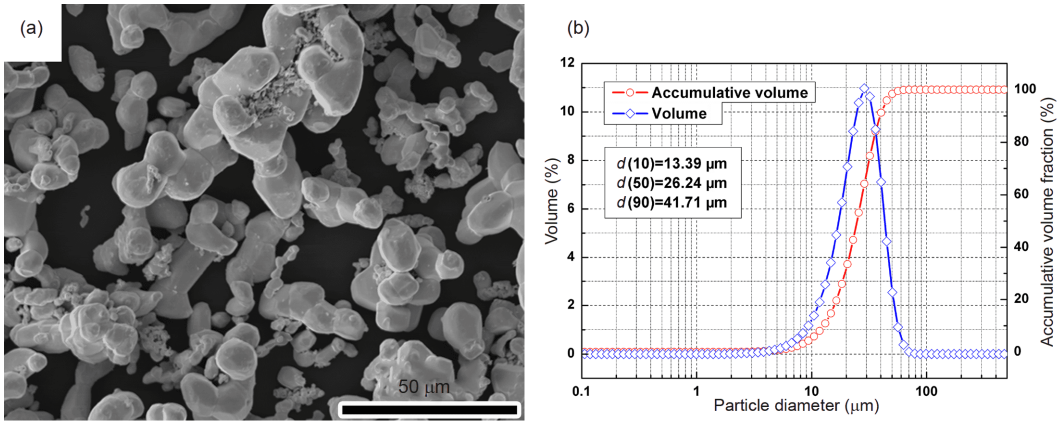

Figure 1 (Color online) SEM morphology (a) and size distribution (b) of Ta powders.

2.2 Cold spray process

Ta powders were deposited on the Ti6Al4V substrate using cold spray equipment assembled by our research group. This equipment consisted of a standard De Laval (convergent-divergent) nozzle possessing the rectangular cross-section exit with an aperture of 2 mm×10 mm and a rectangular throat of 2 mm×3 mm. Compressed air was used as the accelerating gas as well as the carrier gas. During the cold spray process, the temperature was maintained at (450±10)°C and the primary gas pressure was kept at (2.2±0.2) MPa. The standoff distance from nozzle exit to substrate surface was fixed at 20 mm. The spray gun was moved at a line speed of 2 mm/s above the substrate. The powder feed rate was approximately controlled in 50 g/min.

2.3 Microstructure characterization

The laser confocal scanning microscope was used to observe the holes on the sample surface. The microstructures of surface and cross section for the as-sprayed Ta coatings were investigated by SEM. The coating porosity was determined by quantitative image analyses on plenty of SEM cross-section photos. X-ray diffraction (XRD) analyses of the powders and as-sprayed coatings were performed. Finally, Vickers microhardness measurements were on the cross-section of the coated samples with a load of 100 g for 15 s.

2.4 Adhesive bonding strength

The bonding strength between the coating and the substrate was determined using a tensile adhesive test [51]. The term of "adhesive bonding strength", which refers to the bonding between the coating and the substrate, is used in the present work. To measure the adhesive bonding strength, cold sprayed coating was deposited at one side of the cylindrical substrate (Φ20 mm×5 mm) and the other side of the cylindrical substrate was ground and gritted. Then both sides were glued to cylindrical sticks using E-7 epoxy glue. The tensile test was conducted at a cross-head speed of 0.5 mm/min. The nominal tensile adhesive bonding strength was defined as the peak load at yield divided by the area of the coating/substrate interface. All the tests were carried out in air at room temperature.

2.5 *In vitro* bioactivity

The simulated body fluid (SBF) test [52] was adopted for a preliminary bioactivity evaluation. The SBF solution, whose composition nearly equal to those of human blood plasma is given in Table 1, was produced using analytical reagent of NaCl, $NaHCO_3$, KCl, $K_2HPO_4{\cdot}3H_2O$, $MgCl_2{\cdot}6H_2O$, $CaCl_2$ and Na_2SO_4, which were dissolved in deionized water and buffered using tris-hydroxymethyl aminomethane ($(CH_2OH)_3CNH_2$) buffer and 1.0 M HCl to pH of 7.4 at 36.5°C. Samples were soaked in 10 mL SBF at 36.5°C and 5 mL of SBF were removed from each sample every 2 days and replaced with new SBF. After expected time, samples were removed from SBF solution, and gently washed with deionized water followed by drying in a clean container at room temperature. The sample morphology and elemental composition were observed by SEM and energy-dispersive spectroscopy (EDS).

Table 1 Nominal ion concentrations of SBF in comparison with those in human blood plasma

Ion	Ion concentrations (mM)	
	Blood plasma	SBF
Na^+	142.0	142.0
K^+	5.0	5.0
Mg^{2+}	1.5	1.5
Ca^{2+}	2.5	2.5
Cl^-	103.0	147.8
HCO^{3-}	27.0	4.2
HPO_4^{2-}	1.0	1.0
SO_4^{2-}	0.5	0.5
pH	7.2–7.4	7.4

3 Results and discussion

3.1 Microstructure of cold sprayed tantalum coatings

Figure 2 shows the surface morphology of cold sprayed samples. It is found that the surface of the cold sprayed Ta coating is uniformly distributed with some large visible holes, and rough surface formed by accumulation of Ta particles can be seen around the holes. Using image analysis software, the percentage of these holes is about 43%. Through the laser confocal image, many micron-size holes whose diameter and depth are about 200 and 250 μm respectively can be intuitively seen on the surface of the cold sprayed Ta coatings. Researches proved that osteoblasts can grow in the pore whose diameter is 100–200 μm [53]. So the porous surface of the Ta coating may be beneficial to bone ingrowth.

It is well-known that, in the process of cold spray deposition, the high-velocity particles impact the substrate and then produce serious plastic deformation, resulting in the bonding [54–57]. The adhesion of particles in this process is due solely to their kinetic energy upon impact. It has been recognized that the bonding mechanism is adiabatic shear instability proposed by Assadi in 2003 [58]. Experimental investigations show that successful bonding is achieved only above a critical particle velocity, whose value depends on the

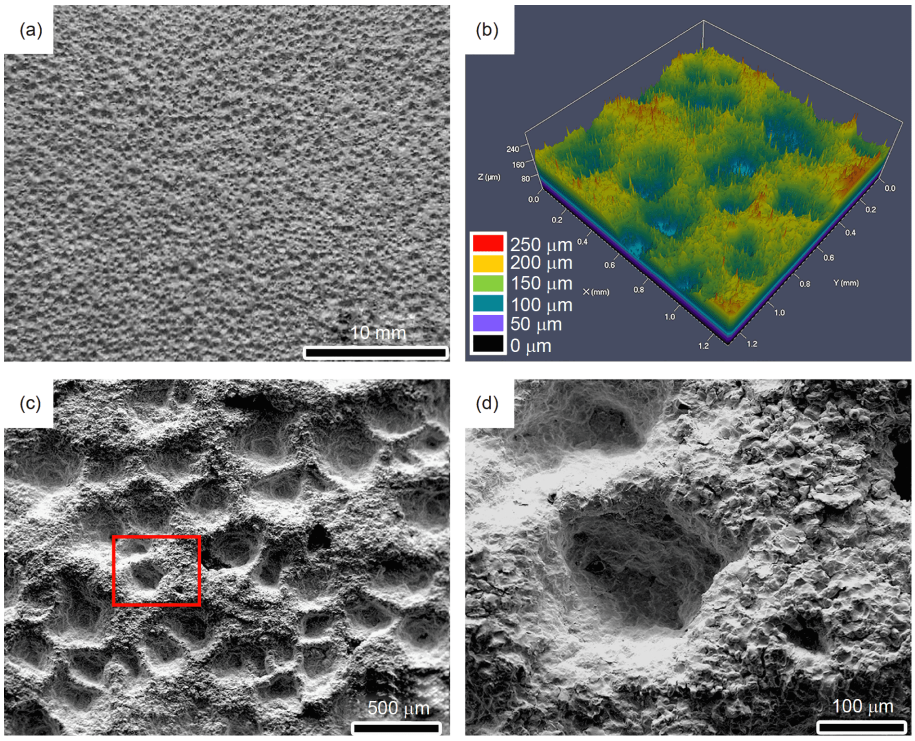

Figure 2 (Color online) Surface morphology of cold sprayed Ta coatings. (a) Macroscopic; (b) laser confocal image; (c) SEM micrographs; (d) high magnification of (c).

temperature and properties of the sprayed material [58,59].

$$v_c = 667 - 14\rho + 0.08T_m + 0.1\sigma_u - 0.1T_0, \quad (1)$$

where v_c is a critical velocity in m/s, ρ is the density in g/cm^3, T_m is the melting temperature in °C, σ_u is the ultimate strength in MPa and T_0 is the initial particle temperature in °C. Therefore, the difference of cold spray deposition would be reflected in the difference of critical velocity caused by the difference of various factors. Among them, the most common one to improve the deposition quality is by improving the spraying parameters (such as temperature and pressure) [60–62]. In addition, based on our recent researches, it was found that the morphology of feedstock powder could significantly affect the deposition behavior from the source [63]. The idea behind this work is to get a rough/porous surface structure with lots of pores, which would contribute to our subsequent improvements in biological performance.

In fact, these holes on the surface are cone-shaped in cold spraying process and its cross-section is shown in Figure 3(a). It was speculated that the formation of these cone-shaped holes was due to the poor cold spray ability of such Ta powder [63]. For example, when they impacted onto the substrate, it could not reach the adiabatic shear instability required for particle bonding and lead to rebound due to insufficient particles' kinetic energy. That was an initiation of cone-shaped hole.

In the process of cold spraying, there would be a certain thickness shock layer on the surface of a flat substrate [64–66]. If a hole appeared on the surface of the sample, it was equivalent to thickening the shock layer at holes' position. Particle impact velocity would decrease drastically owing to strong deceleration by viscous drag behind the shock wave [67,68]. There was no doubt that these particles could not be able to penetrate the additional shock layer. It was reported that as the hole became narrower and deeper, the ratio of particles with final impacting velocity higher than the critical velocity became lower [69]. Then the deposition efficiency inside the hole was lower than that of the plane substrate. Thus the deposition efficiency difference between the hole and substrate led to different thickness growth rate. As the thickness of coatings increased, the holes were magnified, resulting in the visible cone-shaped holes.

Figure 3(a) shows cross-section of the cold sprayed Ta coating on Ti6Al4V substrate. Here it can be further observed the relatively even distribution of cone-shaped holes as mentioned above. It is found that the thickest region of coating is about 380 μm and the thinnest region is about 24 μm (Figure 3(b)). From Figure 3(c), it can be seen that there are many pores in the outer part of the coating. The calculated porosity is about 11%. From Figure 3(d), it is found that the inner part of the coating is denser than the outer part. The porosity inside the coating is significantly reduced to only 2%. This is mainly because that the outer part of the coating is lack of subsequent hammering of particles [70]. From the interface between coating and substrate as shown in Figure 3(e), the bonding largely originates from

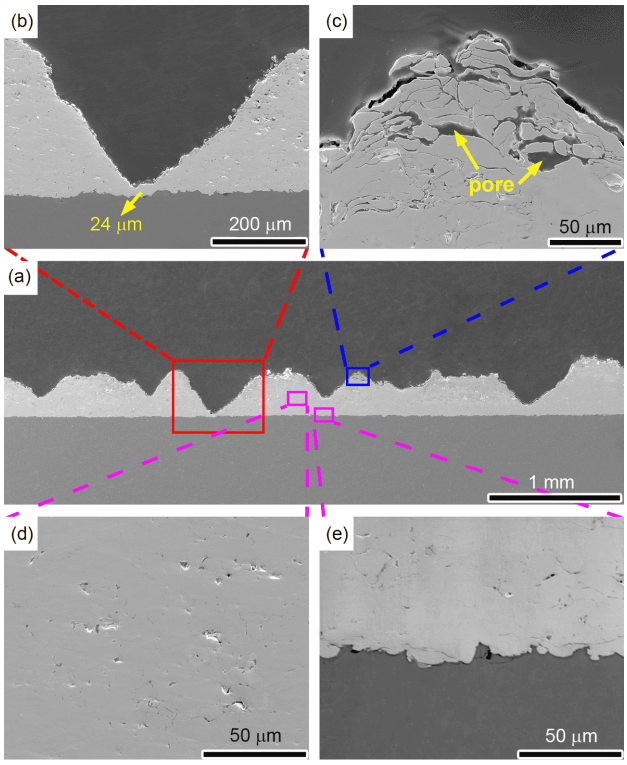

Figure 3 (Color online) Cross-section morphology of cold sprayed Ta coatings. (a) Overview; (b) cone-shaped hole; (c) outer part; (d) inner part; (e) substrate/coating interface.

mechanical interlocking between the Ta particles and the substrate. These results indicate that the cold sprayed Ta coating has a rough/porous surface including some holes. This porous structure may be beneficial to increase the bonding of the implant surface to human bone cells as well.

3.2 XRD analysis

Figure 4 is the XRD spectrum of the original Ta powder and as-sprayed Ta coating. It shows that cold sprayed Ta coating can be very good to keep the nature of the raw material of Ta powder. Namely, Ta powder crystal structure did not change during the cold spraying process, and the coating did not appear obvious oxidation phenomenon. Therefore, it is indeed a simple and effective method of preparing tantalum coating by cold spraying.

3.3 Microhardness

The microhardness of the cold sprayed Ta coating in this paper is found to be about 300 $HV_{0.1}$ on average in the inner part. Microhardness of 350 $HV_{0.1}$ and 135 $HV_{0.1}$ was reported for Ta coatings deposited using angular powder [49] and spongy powder [26], respectively. It could be seen that the microhardness of cold sprayed Ta coating is determined by the difference of Ta powders. The coating using spongy Ta powder would have a lower microhardness value because of its internal loose and porous structure. For the cold sprayed coating using dense Ta powder, it would have a higher microhardness value. What is more, the structure of the cold sprayed Ta coating is not uniform, so the microhardness value with the depth of coatings presents a distribution trend of what is shown in Figure 5. The bigger value is due to the relatively denser inner, while the loose and porous area in the outer part of the coating shows a significantly smaller hardness value (Figure 6).

Compared with the microhardness values of the cold worked (200 $HV_{0.1}$) and annealed (100 $HV_{0.1}$) bulk Ta [26], it is found that the value of the loose and porous area of the as-sprayed Ta coating is between the reported values of cold worked and annealed bulk Ta. Differences in microhardness between Ta coating and bulk Ta are because work hardening and porosity simultaneously exist in Ta coating. During spraying, deposited Ta coatings could be impacted by subsequent particles. The severer the plastic deformation, the stronger the grain refinement, therefore the microhardness is greater [71]. However, there are some pores in these loose and porous surface areas, thus the microhardness value is low.

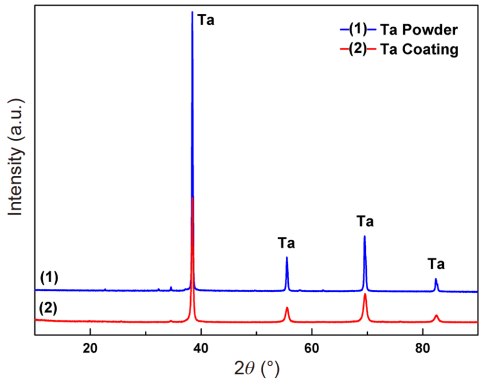

Figure 4 (Color online) XRD patterns of Ta powder and cold sprayed Ta coating.

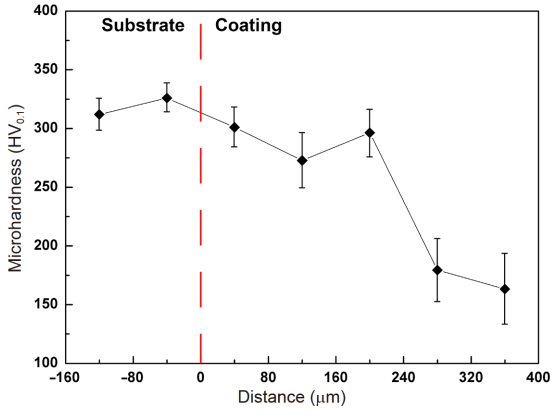

Figure 5 (Color online) Microhardness values with the depth of coating.

3.4 Adhesive bonding strength

Long term integrity is one of the most important issues for the biological implant materials. In this study, through tensile adhesive test, coatings failed by coating/substrate interface failure, and the adhesive bonding strength between the coating and the substrate is about 18.6 MPa. Thus, a possible explanation is that the initiation of the failure is mainly induced by local defects, like porosity, near the coating/substrate interface, which would result in rapid crack propagation and premature interface failure when cracks are subjected to tensile loading such as that applied during tensile pull-off testing. The bonding of the coating and substrate is mainly mechanical interlock. Therefore, further methods should be taken to improve the bonding strength between the cold sprayed Ta coating and the Ti6Al4V substrate.

3.5 *In vitro* biological assessment

The ability of cold sprayed Ta coatings to induce hydroxyapatite (HA) growth in SBF was used as a measure of bioactivity [24]. Figure 7 shows SEM photographs of the surfaces of Ta coatings soaked in SBF for various periods. After 3 days of immersion, a small amount of tiny particles attached to the bottom and inner wall of the cone-shaped holes mentioned above. After samples were soaked in SBF for 2 weeks, the tiny apatite particles on the surface had grown up into spherical particles. Moreover, the apatite sediments could be observed after the samples were removed from SBF and cleaned by deionized water, which indicated that the apatite sediments were not simply attached to the surface but the result of interaction between the sample surface and SBF, as red marked in Figure 7(b). Finally, the sample surface was covered with apatite layer after 4 weeks

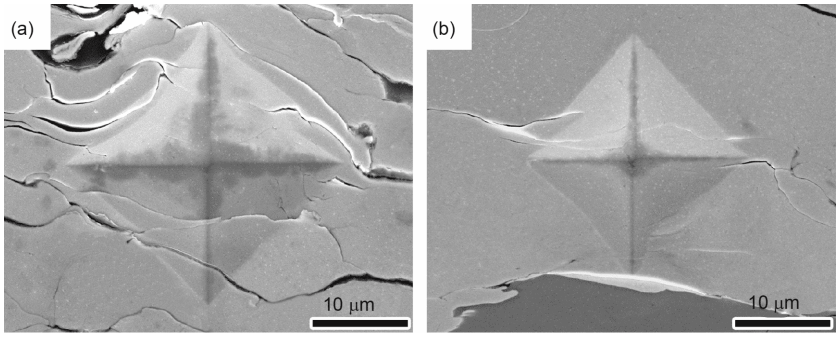

Figure 6 Micro-indentations on the outer (a) and inner (b) of the cross-section of coatings.

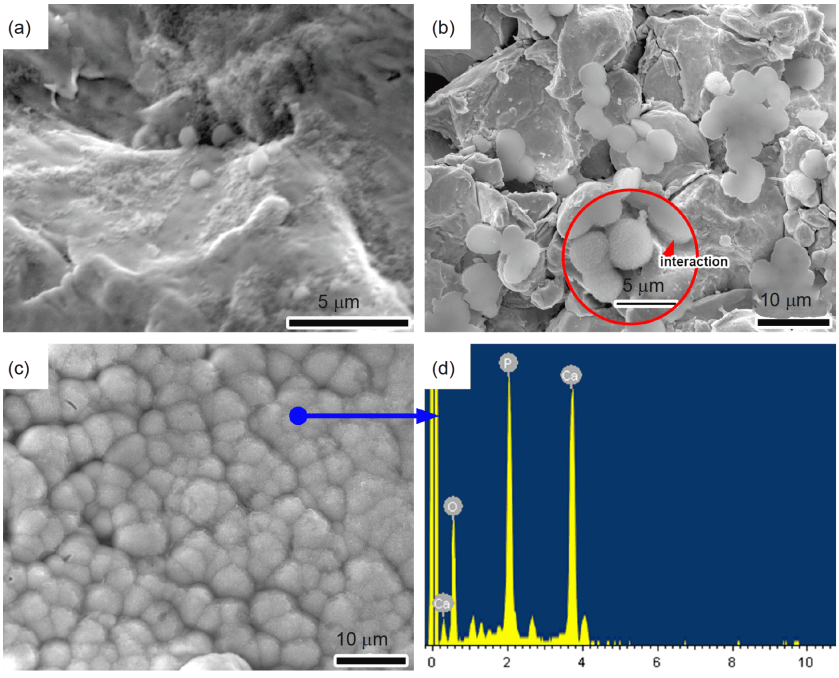

Figure 7 (Color online) SEM photographs of the surfaces of as-sprayed Ta coating after soaking in SBF for 3 days (a), 2 weeks (b), 4 weeks (c) and the corresponding EDS spectrum (d) of 4 weeks.

of immersion (Figure 7(c)). As the corresponding EDX spectrum shows, Ca and P peaks were strong. In addition, compared to other references [72,73], the Ti6Al4V substrate did not show any signs of apatite particle formation after soaking in SBF for 3–14 days, or even one month. It is found that the cold sprayed Ta coating in this work has better ability to induce apatite mineralization than the Ti6Al4V substrate.

Human blood plasma is supersaturated with respect to hydroxyapatite even in normal condition. This means that apatite crystal can spontaneously grow once apatite nuclei would be formed in such an environment. Therefore, after the preparation of rough/porous Ta coating by cold spraying on Ti alloy substrate, the difference on the rate of apatite formation is attributed to the ability of induction of heterogeneous nucleation on the surface [74]. Based on the present results, it is found that the heterogeneous nucleation of apatite is related to two factors: one is that Ta has better biological properties than Ti; the other is that it benefits from the rough/porous surface structure produced by cold spraying. It has been reported that the process is listed for the apatite formation in SBF as follows [24]: (1) Ta-OH groups are formed on the surface of Ta metal; (2) The formed Ta-OH groups first combines with small amount of Ca^{2+} ions; (3) Then combines with PO_4^{3-} ions; (4) Large amount of Ca^{2+} ions and PO_4^{3-} ions are later adsorbed onto the surface of Ta metal to form apatite.

It is found that apatite particles are initially formed in the hole, so it is reasonable to believe that Ta-OH is initially enriched in the hole and then gradually develops outward. Researches [24,75] indicate that the formation of Ta-OH groups governs the rate of the apatite nucleation on the surface of Ta and relies on the adsorption and enrichment of OH- on the coating surface, prompting the precipitation dissolving balance in the solution of hydroxyapatite (2) move to the left and mineralization of apatite particles on the surface.

$$Ca_{10}(PO_4)_6(OH)_2 \rightleftharpoons 10Ca^{2+}+6PO_4^{3-}+2OH^- \quad (2)$$

In addition, it has been reported that implant surface roughness plays a role in determining phenotypic expression of cells *in vivo* [76] and the cell adhesion depends on the available surface area [77]. Rough and porous surfaces have emerged as versatile biomaterials for enhancing fixation to bone [78–80]. Through the present work, it has been observed that porous/rough Ta coatings can be obtained by cold spraying. Besides, the upper part of the coating also provides certain porosity due to little subsequent tamping effect and then the insufficient deformation of the particles, which could be beneficial for osseointegration and cell attachment. The remaining surface micro-features given by feedstock topography could play a role on the cell adhesion and proliferation [79]. Further details on this point should be investigated elsewhere in order to reveal general principles on how cold sprayed Ta surface induced the apatite nucleation in body environment. As a result of the extremely rough/porous Ta coatings, early integration of bone tissue with Ta-coated implants may occur.

4 Conclusion

A rough/porous Ta coating has been successfully fabricated by cold spraying on Ti6Al4V substrate. The experimental results showed that this process had the potential to create rough/porous Ta coatings without obvious oxidation transformation, and further methods were needed to improve the lower bonding strength. The rough surface of the coating with lots of visible holes may be beneficial for the attachment, proliferation and functional expression of osteoblasts. The microhardness of the inner part of coating was higher than that of pure Ta, which was work hardened by cold spraying, and the microhardness of the outer part of coating was lower due to high porosity. Last but not least, the SBF soaking test showed that spherical apatite sediments were mineralized on rough/porous surface in SBF after 2–4 weeks, which indicated that the cold sprayed Ta coating had good bioactivity. This rough/porous surface was effective for the apatite nucleation on it and may have high potentials for design on novel biomaterials with bone-bonding ability.

1 Loi F, Córdova L A, Pajarinen J, et al. Inflammation, fracture and bone repair. Bone, 2016, 86: 119–130
2 Oryan A, Alidadi S, Moshiri A, et al. Bone regenerative medicine: Classic options, novel strategies, and future directions. J Orthop Surg Res, 2014, 9: 18
3 Chen Q, Thouas G A. Metallic implant biomaterials. Mater Sci Eng-R-Rep, 2015, 87: 1–57
4 Arabnejad S, Burnett Johnston R, Pura J A, et al. High-strength porous biomaterials for bone replacement: A strategy to assess the interplay between cell morphology, mechanical properties, bone ingrowth and manufacturing constraints. Acta Biomater, 2016, 30: 345–356
5 Manam N S, Harun W S W, Shri D N A, et al. Study of corrosion in biocompatible metals for implants: A review. J Alloys Compd, 2017, 701: 698–715
6 Tang T T, Qin L. Translational study of orthopaedic biomaterials and devices. J Orthop Transl, 2016, 5: 69–71
7 Niinomi M. Mechanical properties of biomedical titanium alloys. Mater Sci Eng A, 1998, 243: 231–236
8 Bandyopadhyay A, Espana F, Balla V K, et al. Influence of porosity on mechanical properties and *in vivo* response of Ti6Al4V implants. Acta Biomater, 2010, 6: 1640–1648
9 Nordström E G, Sánchez O M. Physics of bone bonding mechanism of different surface bioactive ceramic materials *in vitro* and *in vivo*. Biomed Mater Eng, 2001, 11: 221–31
10 Ramaswamy Y, Wu C, Dunstan C R, et al. Sphene ceramics for orthopedic coating applications: An *in vitro* and *in vivo* study. Acta Biomater, 2009, 5: 3192–3204
11 Perl D P, Brody A R. Alzheimer's disease: X-ray spectrometric evidence of aluminum accumulation in neurofibrillary tangle-bearing neurons. Science, 1980, 208: 297–299
12 Asri R I M, Harun W S W, Samykano M, et al. Corrosion and surface modification on biocompatible metals: A review. Mater Sci Eng-C, 2017, 77: 1261–1274

13 Niinomi M, Nakai M, Hieda J. Development of new metallic alloys for biomedical applications. Acta Biomater, 2012, 8: 3888–3903
14 Ding D, Xie Y, Li K, et al. Improved mechanical compatibility and cytocompatibility of Ta/Ti double-layered composite coating. Met Implants, 2017, 26: 1292–1300
15 Balla V K, Banerjee S, Bose S, et al. Direct laser processing of a tantalum coating on titanium for bone replacement structures. Acta Biomater, 2010, 6: 2329–2334
16 Levine B R, Sporer S, Poggie R A, et al. Experimental and clinical performance of porous tantalum in orthopedic surgery. Biomaterials, 2006, 27: 4671–4681
17 Bobyn J D, Poggie R A, Krygier J J, et al. Clinical validation of a structural porous tantalum biomaterial for adult reconstruction. J Bone Joint Surgery, 2004, 86: 123–129
18 Wang Q, Qiao Y, Cheng M, et al. Tantalum implanted entangled porous titanium promotes surface osseointegration and bone ingrowth. Sci Rep, 2016, 6: 26248
19 Robin A, Rosa J L. Corrosion behavior of niobium, tantalum and their alloys in hot hydrochloric and phosphoric acid solutions. Int J Refractory Met Hard Mater, 2000, 18: 13–21
20 Chandrasekharan R, Park I, Masel R I, et al. Thermal oxidation of tantalum films at various oxidation states from 300 to 700°C. J Appl Phys, 2005, 98: 114908
21 Burke G L. The corrosion of metals in tissues and an introduction to tantalum. Can Med Assoc J, 1940, 43: 125–128
22 Zhou Y L, Niinomi M, Akahori T. Effects of Ta content on Young's modulus and tensile properties of binary Ti-Ta alloys for biomedical applications. Mater Sci Eng-A, 2004, 371: 283–290
23 Kokubo T, Kim H M, Kawashita M. Novel bioactive materials with different mechanical properties. Biomaterials, 2003, 24: 2161–2175
24 Miyazaki T, Kim H M, Kokubo T, et al. Mechanism of bonelike apatite formation on bioactive tantalum metal in a simulated body fluid. Biomaterials, 2002, 23: 827–832
25 Matsuno H. Biocompatibility and osteogenesis of refractory metal implants, titanium, hafnium, niobium, tantalum and rhenium. Biomaterials, 2001, 22: 1253–1262
26 Van Steenkiste T, Gorkiewicz D W. Analysis of tantalum coatings produced by the kinetic spray process. J Thermal Spray Tech, 2004, 13: 265–273
27 Liu J, Chang L, Liu H, et al. Microstructure, mechanical behavior and biocompatibility of powder metallurgy Nb-Ti-Ta alloys as biomedical material. Mater Sci Eng-C, 2017, 71: 512–519
28 Bobyn J D, Stackpool G J, Hacking S A, et al. Characteristics of bone ingrowth and interface mechanics of a new porous tantalum biomaterial. J Bone Joint Surgery British volume, 1999, 81-B: 907–914
29 Kang X T, Li Y N, Li G Z, et al. Effect of sintering temperature on properties of tantalum porous materials. Rare Metal Mater Eng, 2017, 46: 1092–1096
30 Kinos T, Chen S L, Siitonen P, et al. Densification of plasma-sprayed titanium and tantalum coatings. JTST, 1996, 5: 439–444
31 Matson D W, Merz M D, McClanahan E D. High rate sputter deposition of wear resistant tantalum coatings. J Vacuum Sci Tech A-Vacuum Surfs Films, 1992, 10: 1791–1796
32 Balla V K, Bodhak S, Bose S, et al. Porous tantalum structures for bone implants: Fabrication, mechanical and *in vitro* biological properties. Acta Biomater, 2010, 6: 3349–3359
33 Alkhimov A P, Kosarev V F, Nesterovich N I, et al. Method of applying coatings. Soviet Union Patent. SU1618778, 1980
34 Alkhimov A P, Kosarev V F, Papyrin A N. A method of cold gas-dynamic spray deposition. Dokl Akad Nauk SSSR, 1990, 315: 1062–1065
35 Wu X K, Zhang J S, Zhou X L, et al. Advanced cold spray technology: Deposition characteristics and potential applications. Sci China Tech Sci, 2012, 55: 357–368
36 Stoltenhoff T, Kreye H, Richter H J. An analysis of the cold spray process and its coatings. J Thermal Spray Tech, 2002, 11: 542–550
37 Dykhuizen R C, Smith M F. Gas dynamic principles of cold spray. J Thermal Spray Tech, 1998, 7: 205–212
38 Schmidt T, Gärtner F, Assadi H, et al. Development of a generalized parameter window for cold spray deposition. Acta Mater, 2006, 54: 729–742
39 Assadi H, Kreye H, Gärtner F, et al. Cold spraying—A materials perspective. Acta Mater, 2016, 116: 382–407
40 Yin S, Cavaliere P, Aldwell B, et al. Cold spray additive manufacturing and repair: Fundamentals and applications. Additive Manufacturing, 2018, 21: 628–650
41 Tariq N H, Gyansah L, Wang J Q, et al. Cold spray additive manufacturing: A viable strategy to fabricate thick B4C/Al composite coatings for neutron shielding applications. Surf Coatings Tech, 2018, 339: 224–236
42 Raoelison R N, Xie Y, Sapanathan T, et al. Cold gas dynamic spray technology: A comprehensive review of processing conditions for various technological developments till to date. Additive Manufacturing, 2018, 19: 134–159
43 Rokni M R, Nutt S R, Widener C A, et al. Review of relationship between particle deformation, coating microstructure, and properties in high-pressure cold spray. J Therm Spray Technol, 2017, 26: 1–48
44 Tang J, Zhao Z, Liu H, et al. A novel bioactive Ta/hydroxyapatite composite coating fabricated by cold spraying. Mater Lett, 2019, 250: 197–201
45 Vilardell A M, Cinca N, Concustell A, et al. Cold spray as an emerging technology for biocompatible and antibacterial coatings: State of art. J Mater Sci, 2015, 50: 4441–4462
46 Koivuluoto H, Näkki J, Vuoristo P. Corrosion properties of cold-sprayed tantalum coatings. J Therm Spray Tech, 2009, 18: 75–82
47 Koivuluoto H, Bolelli G, Lusvarghi L, et al. Corrosion resistance of cold-sprayed Ta coatings in very aggressive conditions. Surf Coatings Tech, 2010, 205: 1103–1107
48 Koivuluoto H, Honkanen M, Vuoristo P. Cold-sprayed copper and tantalum coatings—Detailed FESEM and TEM analysis. Surf Coatings Tech, 2010, 204: 2353–2361
49 Kumar S, Vidyasagar V, Jyothirmayi A, et al. Effect of heat treatment on mechanical properties and corrosion performance of cold-sprayed tantalum coatings. J Therm Spray Tech, 2016, 25: 745–756
50 Le Guéhennec L, Soueidan A, Layrolle P, et al. Surface treatments of titanium dental implants for rapid osseointegration. Dent Mater, 2007, 23: 844–854
51 Xiong Y, Zhuang W, Zhang M. Effect of the thickness of cold sprayed aluminium alloy coating on the adhesive bond strength with an aluminium alloy substrate. Surf Coatings Tech, 2015, 270: 259–265
52 Kokubo T, Takadama H. How useful is SBF in predicting *in vivo* bone bioactivity? Biomaterials, 2006, 27: 2907–2915
53 Van Bael S, Chai Y C, Truscello S, et al. The effect of pore geometry on the *in vitro* biological behavior of human periosteum-derived cells seeded on selective laser-melted Ti6Al4V bone scaffolds. Acta Biomater, 2012, 8: 2824–2834
54 Zhao Z, Tang J, Du H, et al. *In-situ* chemical interaction in cold-sprayed Zn/Cu composite coating. Mater Lett, 2018, 228: 246–249
55 Deng N, Tang J, Xiong T, et al. Fabrication and characterization of W Cu composite coatings with different W contents by cold spraying. Surf Coatings Tech, 2019, 368: 8–14
56 Grujicic M, Zhao C L, DeRosset W S, et al. Adiabatic shear instability based mechanism for particles/substrate bonding in the cold-gas dynamic-spray process. Mater Des, 2004, 25: 681–688
57 Bae G, Kumar S, Yoon S, et al. Bonding features and associated mechanisms in kinetic sprayed titanium coatings. Acta Mater, 2009, 57: 5654–5666
58 Assadi H, Gärtner F, Stoltenhoff T, et al. Bonding mechanism in cold gas spraying. Acta Mater, 2003, 51: 4379–4394
59 Raletz F, Vardelle M, Ezo'o G. Critical particle velocity under cold spray conditions. Surf Coatings Tech, 2006, 201: 1942–1947
60 Zhou H, Li C, Ji G, et al. Local microstructure inhomogeneity and gas temperature effect in *in-situ* shot-peening assisted cold-sprayed Ti-6Al-4V coating. J Alloys Compd, 2018, 766: 694–704

61 Yin S, Meyer M, Li W, et al. Gas flow, particle acceleration, and heat transfer in cold spray: A review. J Therm Spray Technol, 2016, 25: 1–23
62 Huang R, Fukanuma H. Study of the influence of particle velocity on adhesive strength of cold spray deposits. J Therm Spray Tech, 2012, 21: 541–549
63 Tang J, Zhao Z, Li N, et al. Influence of feedstock powder on microstructure and mechanical properties of Ta cold spray depositions. Surf Coatings Tech, 2019, 377: 124903
64 Takana H, Li H Y, Ogawa K, et al. Computational and experimental studies on cavity filling process by cold gas dynamic spray. J Fluids Eng, 2010, 132: 01302
65 Takana H, Ogawa K, Shoji T, et al. Computational simulation of cold spray process assisted by electrostatic force. Powder Tech, 2008, 185: 116–123
66 Takana H, Ogawa K, Shoji T, et al. Computational simulation on performance enhancement of cold gas dynamic spray processes with electrostatic assist. J Fluids Eng, 2008, 130: 081701
67 Jodoin B, Raletz F, Vardelle M. Cold spray modeling and validation using an optical diagnostic method. Surf Coatings Tech, 2006, 200: 4424–4432
68 Lupoi R, O'Neill W. Powder stream characteristics in cold spray nozzles. Surf Coatings Tech, 2011, 206: 1069–1076
69 Huang G, Wang H, Li X, et al. Study on the growth of holes in cold spraying via numerical simulation and experimental methods. Coatings, 2017, 7: 2
70 Luo X T, Wei Y K, Wang Y, et al. Microstructure and mechanical property of Ti and Ti6Al4V prepared by an in-situ shot peening assisted cold spraying. Mater Des, 2015, 85: 527–533
71 Van Steenkiste T H, Smith J R, Teets R E. Aluminum coatings via kinetic spray with relatively large powder particles. Surf Coatings Tech, 2002, 154: 237–252
72 Kuo T Y, Chin W H, Chien C S, et al. Mechanical and biological properties of graded porous tantalum coatings deposited on titanium alloy implants by vacuum plasma spraying. Surf Coatings Tech, 2019, 372: 399–409
73 İzmir M, Ercan B. Fabrication of micropit structures on Ti6Al4V alloy using fluoride-free anodization for orthopedic applications. J Mater Res, 2019, 34: 1084–1092
74 Ohtsuki C, Kokubo T, Yamamuro T. Mechanism of apatite formation on $CaOSiO_2P_2O_5$ glasses in a simulated body fluid. J Non-Crystalline Solids, 1992, 143: 84–92
75 Miyazaki T, Kim H M, Miyaji F, et al. Bioactive tantalum metal prepared by NaOH treatment. J Biomed Mater Res, 2000, 50: 35–42
76 Martin J Y, Schwartz Z, Hummert T W, et al. Effect of titanium surface roughness on proliferation, differentiation, and protein synthesis of human osteoblast-like cells (MG63). J Biomed Mater Res, 1995, 29: 389–401
77 Rosales-Leal J I, Rodríguez-Valverde M A, Mazzaglia G, et al. Effect of roughness, wettability and morphology of engineered titanium surfaces on osteoblast-like cell adhesion. Colloids Surfs A-Physicochem Eng Aspects, 2010, 365: 222–229
78 Muth J, Poggie M, Kulesha G, et al. Novel highly porous metal technology in artificial hip and knee replacement: Processing methodologies and clinical applications. JOM, 2013, 65: 318–325
79 Vilardell A M, Cinca N, Garcia-Giralt N, et al. Osteoblastic cell response on high-rough titanium coatings by cold spray. J Mater Sci-Mater Med, 2018, 29: 19
80 Boyan B D, Bonewald L F, Paschalis E P, et al. Osteoblast-mediated mineral deposition in culture is dependent on surface microtopography. Calcified Tissue Int, 2002, 71: 519–529